Nanosecond discharge in air in contact with water with various electrical conductivity: electrical characterization and time-resolved imaging

A. Herrmann[1], J. Margot[1] and A. Hamdan[1]

[1] *Groupe de physique des plasmas, Département de Physique, Université de Montréal, 1375 Avenue Thérèse-Lavoie-Roux, Montréal, H2V 0B3, Québec, Canada*

Abstract: This paper investigates the role of water electrical conductivity ($2 \leq \sigma \leq 1000$ µS/cm) on the discharge characteristics and on the propagation dynamics of streamers; this latter is conducted by using 1-ns-time-resolved imaging. The findings can be explained based on the voltage rise time (τ_{pulse}) and the dielectric relaxation time (τ_r). For instance, at higher σ and when $\tau_r < \tau_{pulse}$, the free charges in solution reduce the applied E-field and neutralize accumulated charges at the surface of the solution influencing thus streamer propagation.

Keywords: nanosecond discharge, streamer-liquid interaction, liquid conductivity.

1. Introduction

Streamer discharges are widely studied because of their unique properties making them attractive for many applications [1]. Streamer is a highly reactive discharge channel that is not in thermodynamic equilibrium and has high electric field at its head [2]. Streamer propagation in gaseous medium, including air, is rather well understood, but it quickly becomes a complex phenomenon as soon as it approaches a solid [3] or a liquid surface [4]. Indeed, the properties of the surface, such as its electrical conductivity and dielectric permittivity, strongly influence the streamer dynamics [4]. Although it is a fundamental subject, understanding streamer-surface interaction remains a cornerstone in the context of applications.

Initiated by electronic avalanches, streamers take place if the number of produced electrons is higher than 10^8, i.e Meek's criterion [5]. In these conditions, the E-field produced from electrons-ions separation becomes relatively high (comparable or higher than the applied one) and controls the following steps of streamer propagation, mainly by initiating secondary avalanches close to streamer's head [5]. It is stated that as the streamer approaches the surface, the production rate of photoelectrons decreases significantly leading to a cease of its vertical propagation [6]. Meanwhile, charges accumulate at the surface and produce a radial E-field. If this latter is strong enough, radial avalanches ignite and lead to the formation of radial streamers at or near the surface [6]. In the case of liquid surfaces, streamer propagation is strongly influenced by the liquid properties, mainly electrical conductivity and dielectric permittivity. The former can be controlled by adjusting the concentration of ions in solution, while the latter can be controlled by choosing liquids with different permittivity.

Herein, the influence of water electrical conductivity on the streamer propagation at water surface is presented. In fact, when an E-field is applied to a water with different electrical conductivity, the ions present in solution move and reorganize in response to the E-field [7]. In the context of streamer propagation, such reorganization can significantly influence the E-field near or at the solution's surface and, therefore, the streamer's propagation dynamics [7]. Despite the scarce works on this subject, it is worth noting that Akishev et al. [7] have performed a 2D simulation study and reported the influence of the electrical conductivity (5 or 600 µS/cm) on the propagation of streamer at the surface of dielectric material with $\varepsilon = 81$ (similar to that of water). The authors showed that the increase of the conductivity has led to a decrease of the streamer propagation length, of the surface charge, and of the E-field intensity at the streamer head. More recently, Ning et al. [8] have simulated the propagation of a streamer discharge in air around a droplet and have showed that an increase of the droplet's electrical conductivity causes a reduction of the space charge field at the streamer's head.

In this work, we conduct an experimental study to investigate the propagation of streamers at the surface of water with various electrical conductivities. The discharges are produced by single shot nanosecond high voltage, and they are characterized electrically as well as by time-resolved imaging with a 1-ns-temporal resolution.

2. Experimental setup

The experimental setup used is shown in Fig. 1. A nanosecond positive pulsed power supply (NSP 120-20-P-500-TG-H, Eagle Harbor Technologies) was used to ignite an electrical discharge in air in contact with water solution. The pulse's plateau was fixed at 100 ns, and the voltage magnitude (V_a) was adjusted between 14 and 20 kV.

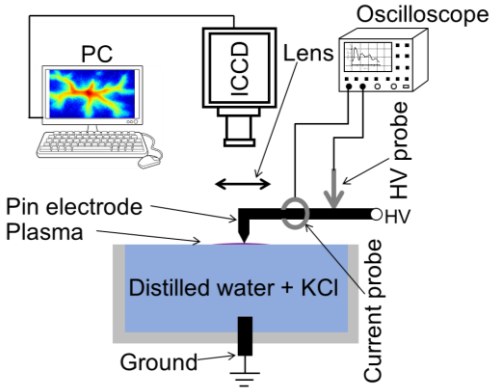

Fig. 1. Scheme of the experimental setup.

The electrical conductivity of the solution (σ) was adjusted between 2 and 1000 µS/cm by adding KCl to deionized water. The anode was a tungsten rod (diameter of 1 mm) with a sharp pin. The gap distance (d) between

the pin and water surface was also adjusted between 10 and 1000 µm using a micrometer positioning displacement system. The cathode was made of a stainless-steel rod (4 mm diameter) placed at the bottom of a cylindrical Teflon cell filled with 20 mL of solution.

3. Results and discussion

3.1. Electrical characterization

Fig. 2 shows the voltage waveforms for typical discharges produced at V_a = 14 and 20 kV and under various σ. We note that the voltage plateau value decreases when σ is increased. Also, σ influences the falling period of the pulse with a more rapid fall at higher σ. These effects are related to the presence of charged species in the solution at higher σ, which modifies the global electrical circuit. Considering the low reproducibility of these discharges, a statistical approach has been conducted during data analysis. Therefore, for a given condition of σ and V_a, the waveforms of hundreds of discharges were acquired, and the data are automatically processed using a home-made algorithm. The outputs are numerous but here we focus on two: i) the breakdown voltage (V_{bk}) and ii) the discharge delay (τ_{pulse}). The magnification in Fig. 2 shows the breakdown moments that are characterized by a voltage drop, and τ_{pulse} corresponds to the discharge delay between the moment of voltage application (t = 0) and the breakdown moment.

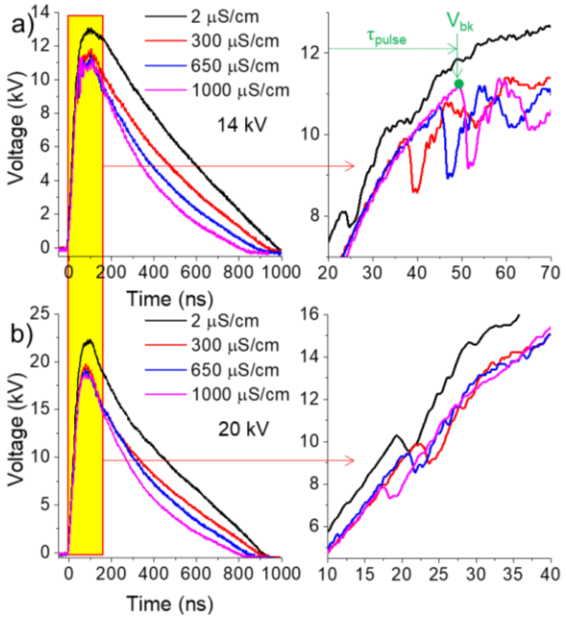

Fig. 2. Voltage waveforms for typical discharges in contact with solution at different σ and at a) V_a = 14 kV and b) V_a = 20 kV.

Fig. 3 shows the variation of V_{bk} as a function of σ at V_a = 14 and 20 kV; d was 400 µm. In the figures, the individual data (black squares) are shown as well as the average value with standard variation (red circles). Depending on V_a, we observe two distinct behaviours. In fact, we performed the measurements for other V_a values between 8 and 20 kV, and the two mentioned behaviours occur for $V_a \leq 14$ kV and $V_a \geq 18$ kV, respectively. Between 14 and 18 kV, a transition-like behaviour is observed. Therefore, we show here only these two typical cases of V_a (14 and 20 kV). At V_a = 14 kV, we find that V_{bk} (average value) is ~8 kV at σ = 2 µS/cm, and it increases with σ to reach a plateau at ~11 kV for σ ≥ 650 µS/cm. We note that this trend was observed at different distances (not shown here), and we found that V_{bd} are lower at shorter d and higher at longer d. At V_a = 20 kV, the trend is reversed. Indeed, V_{bk} is high at low σ and slightly lower at high σ. For instance, at σ = 2 and 300 µS/cm, one measures V_{bk} of ~9.5 kV that decreases to ~8 kV at σ = 650 and 1000 µS/cm.

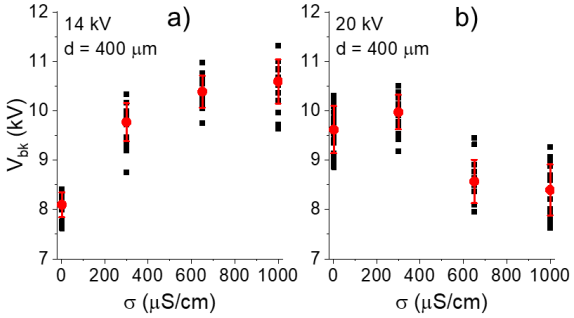

Fig. 3. Variation of V_{bk} as a function of σ at a) V_a = 14kV and b) V_a = 20kV.

These trends can be explained by considering two factors: i) the characteristics of the high-voltage pulse and ii) the characteristics of the solution. In fact, the high voltage pulse is characterized by its rising period τ_{pulse}. As a breakdown will eventually happen after application of the high voltage, τ_{pulse} is then considered the period until a breakdown is observed. Breakdown moments have been identified for all the discharges performed under different conditions, and the obtained average values of τ_{pulse} are summarized in Table 1.

Table 1. Values of τ_{pulse}, at V_a = 14 and 20 kV, and τ_r for different σ values.

σ (µS/cm)	τ_{pulse} V_a = 14 kV	τ_{pulse} V_a = 20 kV	τ_r
2	15-20 ns	13-17 ns	3540 ns
300	27-32 ns	15-18 ns	24 ns
650	30–37 ns	11-15 ns	11 ns
1000	30-37 ns	11-15 ns	7 ns

On the other hand, the dielectric relaxation time of water (τ_r) depends on σ through the following equation [8]:

$$\tau_r = \frac{\varepsilon_r \varepsilon_0}{\sigma} \quad (1)$$

ε_r and ε_0 are the relative dielectric permittivity of water (~80) and the dielectric permittivity of vacuum (~8.85×10-12 F/m), respectively. The values of τ_r for different σ values are also shown in Table 1. τ_r corresponds to the characteristic time to neutralize the space charge field due to the movement of free charges in solution [8]. Thus, it is worth noting that the increase of σ leads not only to a greater concentration of free charges in the liquid, but also

to a decrease of τ_r. In this study, it is thus important to compare τ_{pulse} to τ_r, i.e. Table 1.

In the case of V_a = 14 kV, $\tau_{pulse} < \tau_r$ at σ = 2 µS/cm, which means that the liquid does not have the time to reorganize before the discharge takes place. However, at σ > 300 µS/cm, $\tau_{pulse} > \tau_r$, which means that the liquid does have time to reorganize its free charges. Such an organization results in a decrease of the E-field and, therefore, higher voltage is needed to induce breakdown. The reported results in Fig. 3a agrees with this statement. At V_a = 20 kV, $\tau_{pulse} < \tau_r$ at low σ (2 and 300 µS/cm) and $\tau_{pulse} \sim \tau_r$ for high σ (650 and 1000 µS/cm), i.e. Table 1. Therefore, the liquid does not have the time to reorganize before breakdown occurrence. The slight decrease of V_{bk} (by ~1 kV) with σ can be related to a decrease of the resistivity of the global electrical circuit. Hence, it is feasible to assume that the breakdowns obtained at V_a = 20 kV are equivalent, but the streamer dynamics following the breakdown depend on σ, as clarified hereafter.

3.2. Streamer dynamics

In this section, we show the features of discharge emission at the solution surface acquired using ICCD imaging technique. Two exposure times of the ICCD were used: 50 and 1 ns. The former provides the overall discharge morphology, while the latter show the temporal dynamics of the streamer.

Fig. 4 shows the 50-ns-integrated images of the discharge under these conditions: σ = 2 and 1000 µS/cm and V_a = 14 and 20 kV (d was 200 µm). The pattern of plasma emission clearly depends on the conditions. For instance, at σ = 2 µS/cm and for both V_a (14 and 20 kV), the emission pattern is a disc-like (diameter of ~2 mm) connected to filaments of 2-3 mm that are distributed evenly around the disc. At V_a = 14 kV and σ = 1000 µS/cm, the emission intensity decreases significantly, but it remains possible to distinguish the presence of the disc as well as the organized filaments that have relatively shorter length. At V_a = 20 kV and σ = 1000 µS/cm, the same remarks remain valid, but the intensity of the disc is much higher than that of the filaments. The dependence of the emission on V_a and σ concurs with the results of electrical characteristics. As discussed earlier, at V_a = 14 kV, $\tau_{pulse} < \tau_r$ at σ = 2 µS/cm and $\tau_{pulse} > \tau_r$ at σ = 1000 µS/cm. Therefore, it is expected that the discharge emission at low σ is much higher than that at high σ, because in the latter case the presence of ions in solution can neutralize the charge accumulated at its surface. In the case of V_a = 20 kV, the discharge emission of the disc-like structure remains comparable for different σ cases, but the length and intensity of the organized filaments are significantly reduced. In the case of 1000 µS/cm, as $\tau_{pulse} \sim \tau_r$, the ions in the solution do not have the time to reorganize under the action of the E-field, which results in similar disc-like emission. Concerning the organized filaments that appear several nanoseconds later, in the case of 1000 µS/cm, it seems that the ions in solution do reorganize and neutralize the charge accumulated at solution's surface, which results in a shorter propagation length.

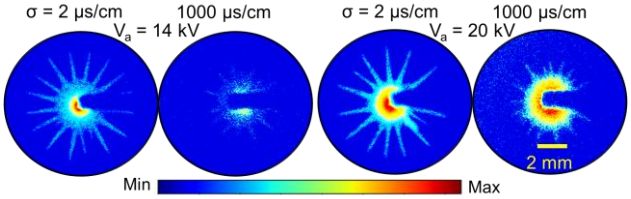

Fig. 4. 50ns-integrated ICCD images of the discharge at the water surface at V_a = 14 and 20 kV and σ = 2 and 1000 µS/cm.

To further investigate the temporal dynamics of the discharge, 1-ns-integrated images were performed under different conditions. The results are shown in Fig. 5. Overall, the evolution of the discharge emission is very similar regardless V_a and σ. In general, the emission starts with a disc-like emission that expands and evolves toward a ring-like structure. Finally, because of the destabilization caused by radial electronic avalanches, the ring splits into plasma dots, which are the head of the streamers. Moreover, the time at which the transition from disc to ring (~3-4 ns) and from ring to dots (~4-5 ns) occur does not significantly depend on V_a and σ. This finding is of interest as it demonstrates that despite the differences in discharge conditions, the dynamics of streamers at the water surface remains comparable. This further supports the assumption that streamers are propagating under the action of space charge field created by charge separation at the streamer's head. However, the total emission lifetime (i.e. propagation length) depends on the conditions. In general, we observed that, the higher is V_a and the smaller is σ, the longer is the propagation length (not shown here). This finding further shows that streamers do interact with the solution and are sensitive to its properties (here electrical conductivity) while propagating. Therefore, it seems that the propagation length is shorter at higher σ due to the reduction of the E-field at water surface because of the presence of charged species in the solution.

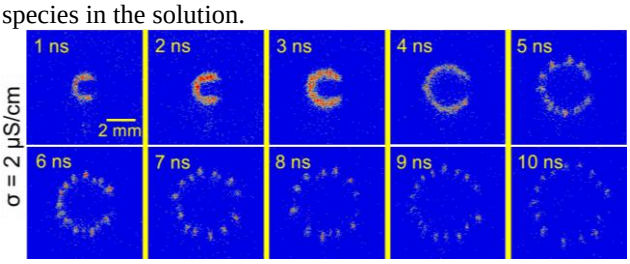

Fig. 5. 1ns-integrated ICCD images of the discharge at the water surface showing its temporal evolution at V_a = 20 kV and σ = 2 µS/cm.

The acquired temporal resolved images (thousands) are then processed using a previously developed algorithm [9] to report i) the instantaneous radial position of plasma dots and ii) their number (N_{dots}). Fig. 6 shows the temporal evolution of the radial position of the plasma dots for V_a = 14 and 20 kV and for σ = 2 and 1000 µS/cm. We note that

at 14 kV the plasma emission remains visible up to ~20 ns at σ = 2 µS/cm, but only up to ~12 ns at higher σ. At V_a = 20 kV, it remains visible up to ~20 ns at σ = 2 µS/cm, while it disappears from ~20 ns at higher σ.

The instantaneous speed of propagation, obtained by temporal derivation of the radial position, is shown in Fig. 6. The initial velocity at σ = 2 µS/cm and V_a = 14 kV is smaller than that at higher σ (~0.3 vs. 0.9 mm/ns). Moreover, the velocity measured in high-σ cases vanishes rather quickly as compared to the low-σ case; this can be related to the neutralization of the space charge in solution as mentioned earlier. In the case of V_a = 20 kV, the influence of σ on the initial propagation velocity is not significant, the breakdowns are similar but, interestingly, the measured values at high σ are lower than those measured in the case of V_a = 14 kV (~0.6 vs. 0.9 mm/ns). This behaviour can be understood by recalling the V_{bd} values. Indeed, at V_a = 14 kV and high σ, V_{bd} is higher than that at V_a = 20 kV (we measured ~10.5 vs. 8 kV, Fig. 3). Moreover, it is also noticeable that the velocity at high-σ cases vanishes relatively quickly as compared to the low-σ case, which agrees with the assumption of ions reorganization after breakdown and neutralization of the accumulated discharge.

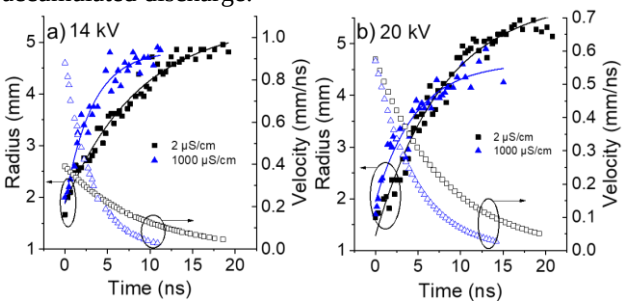

Fig. 6. Temporal evolution of the radial position and the propagation velocity of the plasma dots for σ = 2 and 1000 µS/cm at a) V_a = 14 kV and b) V_a = 20 kV.

The number of plasma dots, determined by processing the images under the different experimental conditions are shown in Figs. 7a and 7b for V_a = 14 and 20 kV, respectively. The data in the figures show the statistical variation as well as the average with standard deviation. At V_a = 14 kV, N_{dots} was rather constant in average (~15) despite the higher V_{bk} measured at high σ. The plasma dots are likely formed by the destabilization of the circular ionization front [9]. In this context, it is expected that the higher is the accumulated charges at solution's surface, the more stable the circular ionization front, the longer the propagation length, and the higher the N_{dots}. Therefore, at V_a = 14 kV, the increase of V_{bk} with σ is likely compensated by the neutralization of accumulated charge by ions in solution. At V_a = 20 kV, N_{dots} decreases quasi linearly from ~20 to ~14 when σ increases from 2 to 1000 µS/cm. This behaviour can be related to a decrease of accumulated charge at the water surface. Although we have previously showed (Table 1) that at V_a = 20 kV and high σ, $\tau_{pulse} \sim \tau_r$, which means that the charged species does not have time to reorganise before breakdown, it is worth noting that the dots are formed several nanoseconds after ignition, which a priori is enough to induce ions movement to neutralize the accumulated charges.

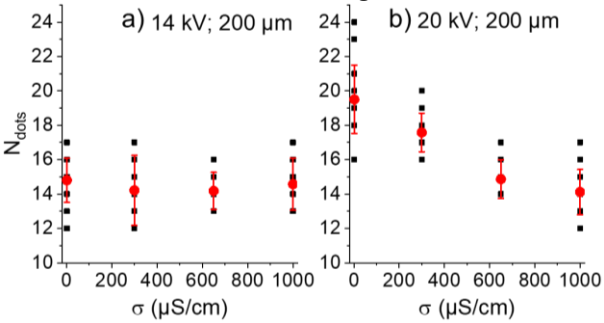

Fig. 7. Variation of N_{dots} as a function of σ at a) V_a = 14 kV and b) V_a = 20 kV.

4.Conclusion

We studied here the formation and propagation of streamers at the surface of solutions with different σ. Depending on V_a and σ, two discharge modes were found. In the case of V_a = 14 kV, V_{bd} increases with σ, while it decreases in the case of V_a = 20 kV. The propagation of discharge at solution surface is also investigated using 1-ns-time-resolved ICCD images. In all conditions, we found that the discharge starts with a disc-like that expands and turns into a ring-like to finally break down into N_{dots} plasma dots. In the case of V_a = 14 kV, we found that N_{dots} does not vary significantly with σ, but it decreases with σ in the case of V_a = 20 kV. The findings reported here can be explained by comparing τ_{pulse} (the delay to observe breakdown) to τ_r (the dielectric relaxation time). In the case of high σ, τ_r is shorter than τ_{pulse}, therefore the charges in solution can move to reduce the applied E-field as well as to neutralize accumulated charges at the surface of the solution.

5.References

[1] M. Keidar et al., Phys Plasmas 20, (2013).
[2] A. Komuro et al., J. Phys. D: Appl. Phys. 47 (2014)
[3] J. Zhang et al., J. Appl. Phys. 128, 093301 (2020).
[4] F. Rezai et al., Applications of Plasma-Liquid Systems: A Review, Materials (2019).
[5] C. Montjin and U. Ebert, J Phys D Appl Phys 39, 2979 (2006).
[6] Q. Z. Zhang et al., Plasma Processes and Polymers 18, (2021).
[7] Y. Akishev et al., Journal of Physics: Conference Series, Vol. 1328 (Institute of Physics Publishing, 2019).
[8] W. Ning et al, Plasma Sources Sci. Technol. 30 (2021)
[9] A. Herrmann et al., Plasma Sources Sci Technol 31, (2022).